doi.org/10.36721/PJPS.2026.39.6.157.1

Jin Ge Fang decoction mitigates alcoholic liver injury in rats via modulation of the TLR4/NF-κB signaling axis

Shuifang Chen, Xuemei Chen, Liangong Peng, Yihui Huang, Yiqing Lin, Yinglian Cai and Qianwen Zheng*
Department of Pharmacy, Xiamen Hospital of Traditional Chinese Medicine, Xiamen, Fujian, China

Abstract: **Background**: Alcoholic liver disease (ALD) poses a significant global health challenge by causing progressive damage due to excessive alcohol consumption, highlighting the urgent need for effective treatments. Jin Ge Fang (JGF) is a traditional formulation whose potential hepatoprotective mechanism remains to be fully elucidated. **Objectives**: This study aimed to investigate the protective effects of JGF on ALD and explore its regulatory roles in oxidative stress, inflammatory cascades, and the Toll-like receptor 4 (TLR4)/nuclear factor kappa-B (NF-κB) pathway. **Methods**: An ethanol-induced ALD rat model was established and assessed histopathologically. Serum levels of hepatic function markers [aspartate transaminase (AST) and alanine transaminase (ALT)] and oxidative stress indicators [malondialdehyde (MDA), superoxide dismutase (SOD), and glutathione peroxidase (GSH-Px)] were measured. Inflammatory cytokines [tumor necrosis factor-α (TNF-α), interleukin-6 (IL-6), and interleukin-1β (IL-1β)] were quantified using enzyme-linked immunosorbent assay (ELISA). Protein expression related to the TLR4/NF-κB pathway was analyzed by Western blotting. **Results**: JGF treatment significantly improved liver histology, reducing steatosis and inflammatory infiltration. It markedly decreased serum AST and ALT activities, suppressed lipid peroxidation (as evidenced by reduced MDA levels), and enhanced endogenous antioxidant defenses (elevated SOD and GSH-Px activities). Furthermore, JGF significantly inhibited the release of pro-inflammatory cytokines (TNF-α, IL-6, and IL-1β) and downregulated the protein expression of key mediators in the TLR4/NF-κB signaling pathway. **Conclusion**: JGF demonstrates significant hepatoprotective effects against ALD. Its benefits are likely mediated through a dual action of ameliorating oxidative damage and suppressing inflammatory activation, potentially via inhibition of the TLR4/NF-κB signaling cascade.

Keywords: Alcoholic liver disease; Inflammation; Jin Ge Fang; Oxidative stress

Submitted on 26-07-2025 – Revised on 06-11-2025 – Accepted on 07-11-2025

INTRODUCTION

Alcoholic liver disease (ALD) spans a spectrum of pathologies from steatosis and hepatitis to fibrosis and hepatocellular carcinoma, representing a major global health burden that accounts for approximately 4% of deaths worldwide (Asrani *et al.*, 2021; Huang *et al.*, 2023). Its incidence is rising, especially among young adults and chronic alcohol users, highlighting an urgent need for effective treatments (Yoo *et al.*, 2024). The pathogenesis of ALD is complicated mechanistically, involving oxidative stress, metabolic dysregulation and immune activation, with the Toll-like receptor 4 (TLR4)/nuclear factor kappa-B (NF-κB) signaling pathway playing a central role in amplifying inflammatory responses and driving hepatic injury (Yang *et al.*, 2022; Kong *et al.*, 2024; Moustafa *et al.*, 2025). Despite progress in understanding these mechanisms, a significant gap remains in the development of targeted therapies for this pathological condition, particularly those derived from traditional botanical medicines.

Traditional Chinese herbal formulas, with multi-target effects and favorable safety profiles, have been extensively investigated and applied in managing ALD (Chen *et al.*, 2025a; Han *et al.*, 2023). Jin Ge Fang (JGF) is a representative formula consisting of *Flos Puerariae*, *Semen Hoveniae*, *Anoectochilus formosanus*, *Poria cocos* and *Citri Reticulatae Pericarpium*, which was developed based on clinical experience and traditional principles. According to the existing data, several components of JGF possess hepatoprotective properties. For example, puerarin from *Flos Puerariae* can reduce oxidative stress and inhibit inflammation, while the active ingredients of *Semen Hoveniae* can promote alcohol metabolism and alleviate hepatic lipid accumulation (Zhang *et al.*, 2023; Li *et al.*, 2025). *Anoectochilus formosanus* also exerts antioxidant and anti-inflammatory activities and both *Poria cocos* and *Citri Reticulatae Pericarpium* have demonstrated regulatory effects on NF-κB signaling and oxidative pathways (Zhou *et al.*, 2024; Jiang *et al.*, 2022; Lee *et al.*, 2022). Currently, the majority of existing studies focus on single herbs. Nevertheless, there is still a poor understanding of the synergistic mechanism of the full JGF formula—particularly its modulation of the TLR4/NF-κB pathway in the context of ALD.

Accordingly, this study was designed to systematically evaluate the hepatoprotective effects of JGF against ALD and to elucidate its underlying mechanisms, with a focus on the TLR4/NF-κB signaling pathway. This study is anticipated to provide comprehensive evidence supporting the potential of JGF as a complementary therapeutic

**Corresponding author:* e-mail: happygirlwater@163.com

strategy for ALD by integrating biochemical assays, histopathological examination and molecular biology techniques in a rat model of ALD.

MATERIALS AND METHODS

Materials

Commercial kits for the detection of aspartate aminotransferase (AST), alanine aminotransferase (ALT), malondialdehyde (MDA), total superoxide dismutase (T-SOD) and glutathione peroxidase (GSH-Px) activities were procured from Nanjing Jiancheng Bioengineering Institute (Nanjing, China). For immunological analyses, enzyme-linked immunosorbent assay (ELISA) kits were supplied by BOSTER Bioengineering Co., Ltd. (Wuhan, China). Key immunological reagents including TLR4 monoclonal antibody, NF-κB p65 recombinant antibody, phospho-NF-κB p65 (Ser468) recombinant antibody and horseradish peroxidase-conjugated secondary antibodies (specifically goat anti-rabbit IgG) were acquired from Proteintech Group, Inc (Wuhan, China). Protein quantification was performed using the bicinchoninic acid (BCA) protein assay kit (Beyotime Biotechnology, Shanghai, China). In addition, in order to ensure consistent quality and composition throughout the study, all the components of JGF were provided by Luyan Pharma Co., Ltd. (Xiamen, China).

The magnetic stirrer was obtained from BKMAMLAB (model: 10L). The dehydration machine, embedding machine, tissue flattener, and freezing station were all supplied by Hubei Xiaogan Kuohai Medical Technology Co., Ltd. (models: KH-TS, KH-BL, KH-P2, and KH-BL, respectively). The microtome was procured from Epredia (model: HM 325). The forced air drying oven was acquired from Shanghai Jinghong Laboratory Equipment Co., Ltd. (model: DHG-9076A). Glass slides were sourced from Jiangsu Shitai Experimental Equipment Co., Ltd. (model: 10128105P-G). The upright optical microscope was provided by OLYMPUS (model: BX41), and the imaging system was from Tupu (model: E31S PM). The refrigerator was supplied by BOSCH-Siemens (model: BCD-254). The vertical slab electrophoresis/transfer apparatus and the electrophoresis instrument were both obtained from Wuhan Servicebio Technology Co., Ltd. (model: SPW-6S). The decolorizing shaker was acquired from Taizhou Nuomi (model: NMYC-60). The 4°C centrifuge was provided by Guangzhou Jidi (model: JIDI-5B). The thermostatic water bath was sourced from Shaoxing Shangyu Xiangda (model: HH600). The grinder was procured from Wuhan Servicebio Technology Co., Ltd. (model: KZ-III). The microplate reader was supplied by Molecular Devices (model: CMax Plus).

Preparation of JGF

Flos Puerariae, *Semen Hoveniae*, *Anoectochilus formosanus*, *Poria cocos* and *Citri Reticulatae Pericarpium* were integrated at a ratio of 10:6:6:10:6 to obtain the mixture that was soaked for 30 min. The initial extraction was performed using a 10-fold water volume with 1.5 h reflux, followed by the secondary extraction with an 8-fold water volume heated for 60 min (Chen *et al.*, 2022). After boiling, the mixture was filtered to get and merge the filtrate for subsequent concentration to the desired level. In use, the crude drugs were diluted in deionized water to adjust the concentrations to 0.21 g/mL and 0.42 g/mL, respectively.

Animal treatment

Sprague-Dawley (SD) rats were housed under standard specific pathogen-free conditions at a controlled temperature of 24~26 °C, relative humidity of 60%~70% and a 12/12-hour light/dark cycle (lights on at 7:00 AM). The model of ALD was established in this study by employing the Lieber-DeCarli rodent model (Cao *et al.*, 2025). Rats in the model group and JGF group underwent a transition phase using Lieber-DeCarli ethanol liquid diet with graded ethanol concentrations (1%→2%→3%→4%) during the first week and were then provided with 5% ethanol liquid diet from the second week onward for 7 consecutive weeks. While animals in the control group received an ethanol-free (substituted with maltodextrin) isocaloric control liquid diet matching the Lieber-DeCarli formulation, as detailed in table 1.

Using a computer-generated random number sequence concealed in sequentially numbered, opaque sealed envelopes, SD rats (180–220 g) were randomly assigned to four treatment groups (n=8 for each group): (1) Vehicle control group; (2) ALD model group; (3) Low-dose JGF (2.1 g/kg); (4) High-dose JGF (4.2 g/kg). All subjects were dosed daily by oral gavage (10 mL/kg). Vehicle controls received volume-matched purified water. Throughout the 8-week study period, JGF decoction was administered concurrently with ethanol exposure as a preventive co-treatment. At the end of the experiment, all rats were euthanized humanely via an intraperitoneal injection of an overdose of sodium pentobarbital (150 mg/kg). Noticeably, no animals were excluded from the study due to accidental death, severe unrelated infections, or failure to complete the intragastric protocol.

Histopathological analysis of liver tissues

The hepatic morphology in experimental rats was evaluated by applying standardized histological techniques. Liver specimens were systematically harvested from the left hepatic lobe of all rats and immediately preserved in 4% paraformaldehyde for 24 hrs to maintain tissue integrity. Subsequent processing steps involved dehydration, paraffin embedding and microtome sectioning sequentially. Histological sections were subjected to standard hematoxylin-eosin (H&E) staining (Jin *et al.*, 2025).

Table 1: The composition of the Lieber–DeCarli alcoholic diet and the control diet.

Content	Lieber–DeCarli Diet	Control diet
Dry mix (g)	132.2	132.2
Water (mL)	817.8	778.2
Anhydrous ethanol (g)	0	89.6
Maltodextrin (g)	50	0

Finally, the histopathological assessment was conducted comprehensively under light microscopy to identify and characterize any structural abnormalities in the hepatic architecture.

Biochemical analysis

Plasma samples from these experimental rats were centrifuged at 3,000 revolutions per minute (rpm) for 20 min under refrigerated conditions (4°C) with a rotor radius of 6 cm. Then, the obtained supernatant serum fraction was meticulously aspirated via precision pipetting. Eventually, the concentrations of ALT and AST were quantitatively determined by employing standardized commercial assay kits to evaluate alcohol-induced hepatic damage.

Oxidative stress factor detection

Liver tissues were weighed (40 mg) and placed in 1.5 mL microcentrifuge tubes for homogenization on ice after the addition of 500 μL extraction buffer. Centrifugation at 10,000 rpm (rcf of 6,700 × g) for 10 min at 4°C (rotor radius of 6 cm) was performed to separate the supernatants, which were stored at 0-4°C for subsequent analysis. Serum preparation followed standardized procedures.

The enzymatic activities of oxidative stress markers (MDA, SOD and GSH-Px) were quantified in both hepatic tissue and plasma samples using commercial assay kits.

Cytokine production assay

Hepatic and circulatory levels of tumor necrosis factor-α (TNF-α), interleukin-1β (IL-1β) and interleukin-6 (IL-6) were quantified via ELISA as instructed. The measurements were performed with eight biological replicates per group and all samples were assayed without dilution as their values fell within the detection range of the standard curve. Initially, samples and standards were added into the pre-coated plate for 90 min of incubation at 37 °C without washing. Subsequently, biotin-conjugated antibody was introduced for another 60 min of incubation at 37 °C, after which the plate was washed three times with 1× wash buffer. Next, avidin-biotin-peroxidase complex was added for 30 min of incubation at 37 °C, after five times of washing, reaction at 37 °C for 25–30 min in the dark was carried out following the application of the tetramethylbenzidine substrate. Finally, the reaction was terminated with stop solution for the measurement of the absorbance at 450 nm.

TLR4/NF-κB pathway-related protein detection

Western immunoblotting was applied to quantify the target protein levels. After homogenization in RIPA buffer (1:10 w/v), these liver samples underwent 20 min of ice-cold lysis. After centrifugation (12,000 × g, 10 min, 4°C), the yielded supernatants were subjected to BCA protein assay for quantification before SDS-PAGE separation on 12% gels.

Furthermore, post-electrophoretic transfer onto PVDF membranes was achieved via semi-dry electroblotting. Membranes were blocked in TBST (0.1% Tween-20) with 5% bovine serum albumin (60 min, room temperature) under continuous agitation. Primary antibodies diluted in blocking buffer were then applied for overnight incubation at 4°C with mild shaking.

After thorough rinsing with TBST, the processed membranes were incubated with HRP-linked secondary antibodies (60 min, room temperature). Enhanced chemiluminescence reagents revealed protein bands, recorded by a digital imaging system. Target protein expression was quantified densitometrically using ImageJ, with the values of optical density normalized to the reference proteins for relative expression analysis.

Statistical analysis

Statistical analyses were performed using GraphPad Prism 8.2.1. Quantitative data were expressed as mean ± standard deviation (SD). Inter-group comparison employed Student's t-test, while multi-group comparison adopted ordinary one-way analysis of variance (ANOVA) followed by Tukey's multiple comparisons test. The assumptions of normality (Shapiro–Wilk test) and homogeneity of variances (Brown–Forsythe test) were verified prior to the ANOVA. A significance threshold of $P < 0.05$ was used throughout the statistical analysis.

RESULTS

JGF reduced histopathological changes of ALD rats

Histopathologically, H&E staining illustrated distinct morphological differences among groups (Fig.1A). The degree of liver tissue damage was assessed by using the Kleiner scoring system (also known as NAS: NAFLD Activity Score) (Cho *et al.*, 2020), with corresponding statistical analysis shown in fig.1B. The control group exhibited preserved hepatic architecture, showing no evidence of lipid accumulation and inflammation. In contrast, the model group demonstrated pronounced hepatic steatosis, manifesting primarily as enlarged

hepatocytes with a ballooning appearance indicative of severe fatty degeneration and inflammation, showing significant difference in the comparison of the NAS value (P=0.0029). Compared with the model group, there was significantly reduced fat accumulation and inflammatory response in both treatment groups (P=0.0075, P=0.0053).

JGF impacted liver function levels in ALD rats

The hepatic biochemical markers were further evaluated comprehensively to highlight the impact of serum aminotransferase concentrations on hepatic function in ALD rats (Fig.1C and 1D). According to the comparative analysis, there was a markedly elevated serum aminotransferase level in the model group compared to the control group (ALT: $P < 0.0001$; and AST: $P = 0.0029$). Administration of low-dose JGF resulted in statistically significant attenuation of ALT elevation ($P = 0.0168$), but no significant decline in the level of AST ($P = 0.9614$). Notably, high-dose JGF treatment demonstrated significant hepatoprotective effects, as evidenced by substantial decreases in both ALT and AST levels ($P = 0.0060$ and $P = 0.0428$). Collectively, JGF exhibits dose-related therapeutic efficacy against ALD.

JGF inhibited oxidative stress in ALD rats

As demonstrated in Fig. 2, compared to the control group, the model group displayed markedly elevated MDA concentrations in both plasma and hepatic tissues ($P = 0.0027$ and $P < 0.0001$, respectively), but substantially diminished activities of SOD and GSH-Px (all $P < 0.05$).

Furthermore, compared with the untreated modeled animals, therapeutic intervention with JGF at both low and high doses resulted in significant attenuation of MDA accumulation (all $P < 0.05$), alongside notable enhancement of antioxidant enzyme activities (all $P < 0.05$). Therefore, JGF administration can effectively ameliorate oxidative stress in ALD rats.

JGF mitigated cytokine production in ALD rats

Our subsequent investigation focused on the quantification of pro-inflammatory cytokine concentrations in both plasma and hepatic tissues via ELISA, with the purpose of unveiling the anti-inflammatory properties of JGF in ALD rats. As depicted in fig. 3, there were dramatically upregulated levels in pro-inflammatory mediators (TNF-α, IL-1β and IL-6) in the modeled rats versus controls (all $P<0.05$). Notably, JGF administration at both low and high doses effectively attenuated these inflammatory mediators, demonstrating statistically significant reductions compared to the untreated modeled animals (all $P <0.05$).

JGF affected TLR4, NF-κB and p-NF-κB protein expression in ALD rats

As demonstrated in Fig. 4, elevated protein expression of TLR4, NF-κB p65 and phosphorylated NF-κB p65 was detected in hepatic tissues from the model group relative to control animals ($P < 0.0001$, $P < 0.0001$, $P = 0.0001$, respectively). Notably, both low-dose and high-dose JGF interventions led to substantial attenuation of these inflammatory mediators 0.05 to $P < 0.0001$ for NF-κB p65 and p-NF-κB p65 across treatment conditions).

DISCUSSION

ALD, also known as alcoholic hepatitis, represents one of the leading causes of chronic liver disease, featuring alcohol-initiated hepatic lesions that progress from steatosis through hepatitis to fibrosis-cirrhosis transformation. The escalating prevalence of ALD is particularly alarming due to its substantial contribution to morbidity and mortality, especially among individuals in their most productive years.

As a well-established process, hepatic metabolism of ethanol can be described as follows: excessive ROS production may be triggered by chronic excessive alcohol consumption, which further induces oxidative stress, impairs mitochondrial function and severely compromises cellular oxidative phosphorylation (Yeh *et al.*, 2023). Moreover, the produced ROS can initiate a pro-inflammatory cascade through the activation of cytokine production, further exacerbating ALD progression (Chen *et al.*, 2025b).

It is well-known that the pathogenesis of ALD involves multiple interconnected mechanisms. Noticeably, current evidence highlights the pivotal roles of oxidative stress, chronic inflammation and dysregulation of the TLR4/NF-κB signaling axis in initiating and promoting ALD development (Zhang *et al.*, 2024; Wang *et al.*, 2025; Farhadi *et al.*, 2025).

In this study, our authors focused on systematically evaluating the hepatoprotective properties of the traditional Chinese medicine JGF in ALD. This study delineated the pleiotropic benefits of JGF through a comprehensive exploration of oxidative biomarkers, inflammatory cascades and TLR4-NF-κB signaling dynamics. Our investigation depended on the establishment of a standardized animal model and employment of rigorous analytical techniques including biochemical parameter assessment and liver tissue histology. Consequently, JGF administration effectively attenuated hepatic injury, enhanced hepatic functional parameters, mitigated oxidative damage and regulated pro-inflammatory cytokine production. Mechanistically, JGF could potently suppress the activation of the TLR4/NF-κB pathway. Eventually, our study underscores JGF as a novel therapeutic candidate for ALD, which merits accelerated clinical translation.

Hepatocytes serve as the primary functional units and the hepatic system has been confirmed to be crucial in maintaining metabolic homeostasis. ALT and AST represent two key biochemical markers for assessing hepatocellular integrity.

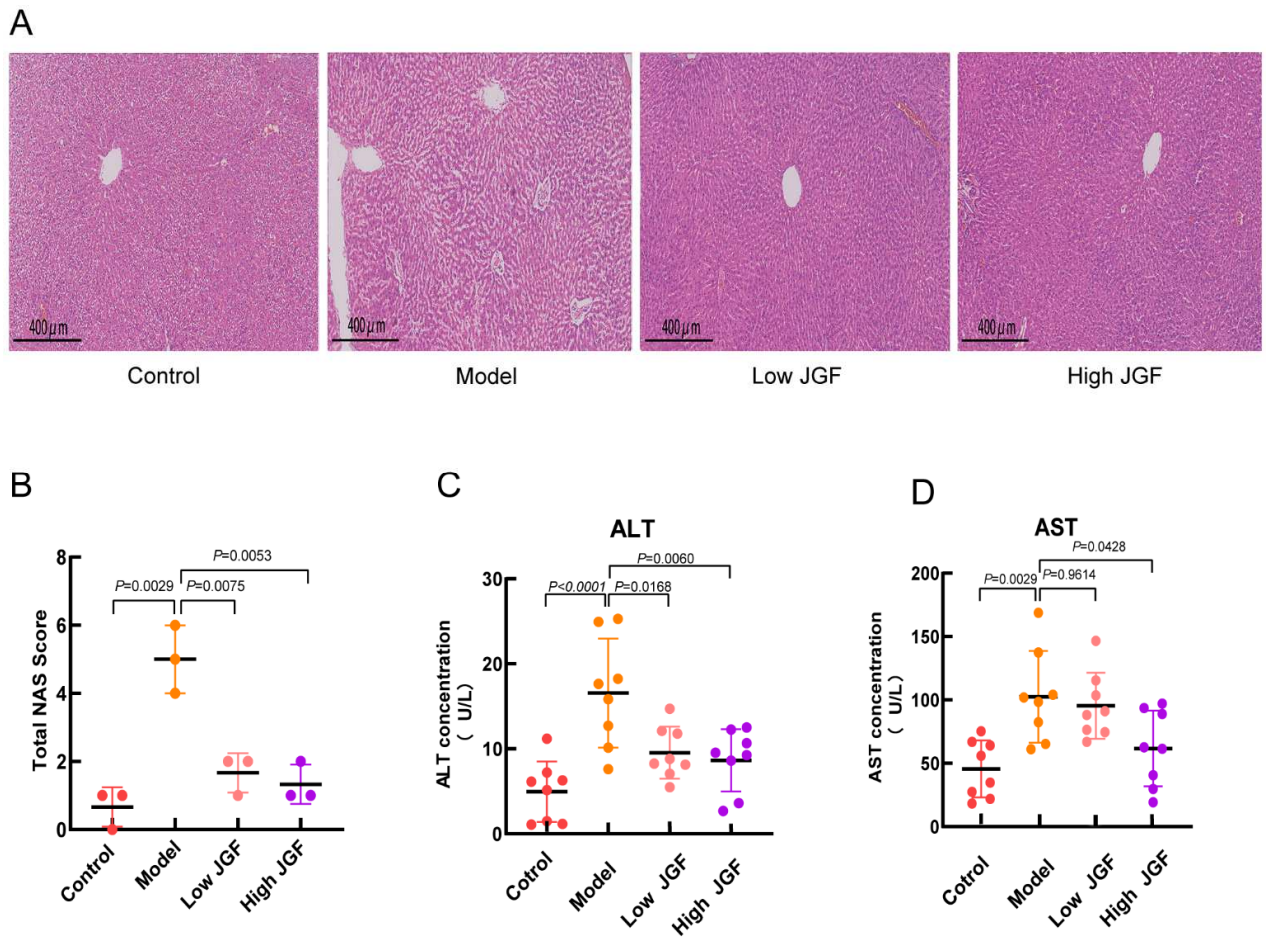

Fig. 1: Pathological sections of liver tissues and effect of JGF on liver function in ALD rats. (A) Pathological imaging (H&E staining ×400). The scales bar represents 400 μm. (B) The scoring results of liver pathology using the Kleiner scoring system. Statistical analysis of NAS value [mean ± SD, n=3] was conducted by using the Kruskal-Wallis non-parametric test combined with Dunn's post-hoc test. (C) ALT in serum. (D) AST in serum. All data of ALT and AST are presented as mean ± SD (n=8) and analyzed via the ordinary one-way ANOVA combined with Tukey's multiple comparisons test. A value of $P < 0.05$ indicates the presence of significant difference.

ALT usually localizes within the cytoplasm of hepatocytes. Its level rises rapidly in response to cellular inflammation or damage, making it a sensitive biomarker for hepatic injury (Laschtowitz *et al.*, 2021). Meanwhile, AST primarily resides within mitochondrial compartments, exhibiting increased concentration in the serum in the case of significant cellular necrosis or damage. Furthermore, elevated levels of proinflammatory mediators may also unveil an augmented systemic inflammatory state.

Histopathological evaluation revealed that the ALD model group exhibited extensive steatosis, a hallmark pathological manifestation of ALD (Cao et al., 2021). This group also showed significant elevations in both ALT and AST activities. Collectively, these data supported a robust construction of our experimental model, furnishing a validated platform for downstream research endeavors and offering compelling evidence for the potent hepatoprotective efficacy of JGF. Hepatic injury mediated by oxidative stress represents a fundamental pathological mechanism underlying ALD. Intracellularly, mitochondria are the principal generators of ROS, which are predominantly neutralized by SOD. Through the promotion of the oxidation of reduced glutathione, GSH-Px can facilitate the conversion of hazardous peroxides into innocuous hydroxyl derivatives, thereby safeguarding cellular membrane integrity against oxidative degradation. Consequently, SOD and GSH-Px, functioning as efficient scavengers of superoxide radicals, constitute the foremost enzymatic defense against oxidative damage (Su *et al.*, 2024). In addition, MDA is the terminal product of lipid peroxidation, which is proposed to be a reliable indicator of oxidative stress, with its tissue concentrations revealing the extent of lipid peroxidative damage (Toto *et al.*, 2022).

In our model of ALD, ethanol challenge triggered sustained ROS elevation, coinciding with depressed SOD and GSH-Px enzymatic function and MDA accumulation.

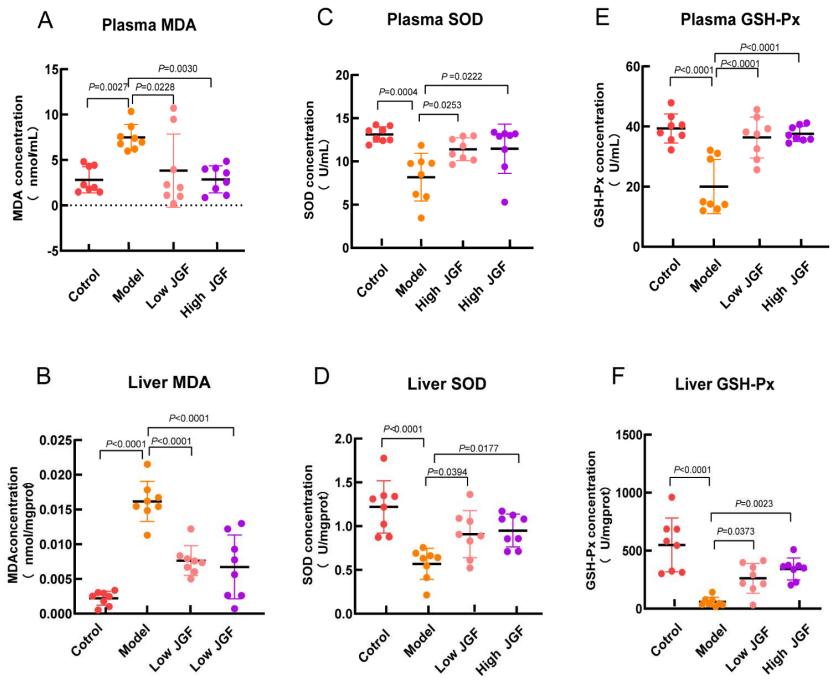

Fig. 2: Effects of JGF on the levels of oxidative stress in ALD rats. (A) MDA in plasma. (B). MDA in liver tissue. (C) SOD in plasma. (D). SOD in liver tissue. (E) GSH-Px in plasma. (F) GSH-Px in liver tissue. All data are presented as mean ± SD (n=8), using ordinary one-way ANOVA combined with Tukey's multiple comparisons test. A value of $P < 0.05$ indicates the presence of significant difference.

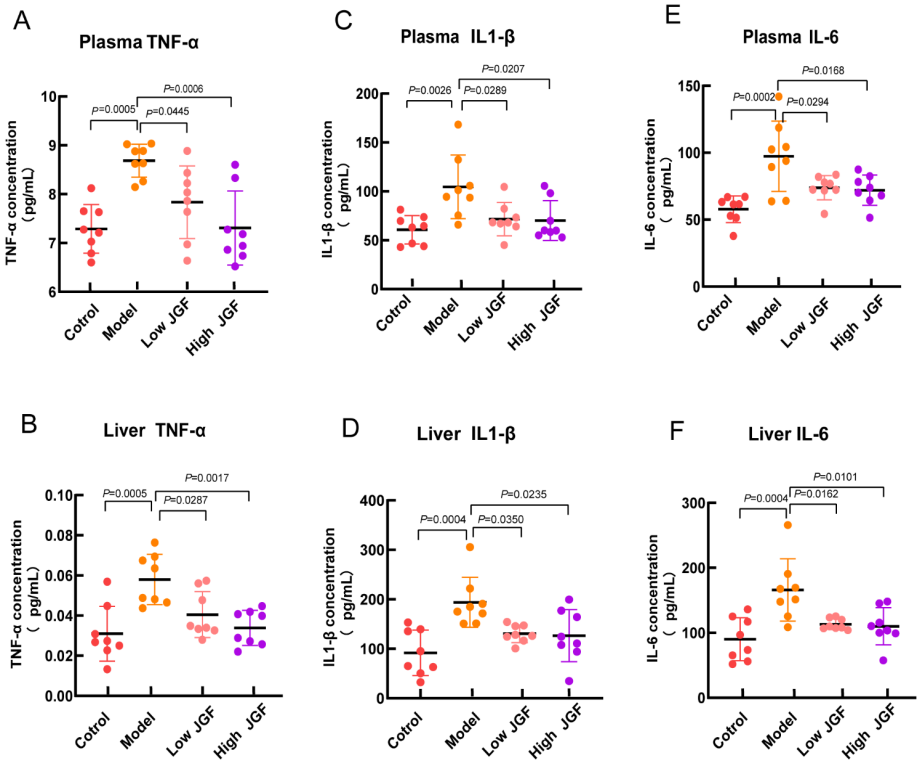

Fig. 3: Effects of JGF on the levels of inflammatory factors in ALD rats. (A) TNF-α in plasma. (B). TNF-α in liver tissue. (C) IL-1β in plasma. (D) IL-1β in liver tissue. (E) IL-6 in plasma. (F). IL-6 in liver tissue. All data are presented as mean ± SD (n=8), using ordinary one-way ANOVA combined with Tukey's multiple comparisons test. A value of $P < 0.05$ indicates the presence of significant difference.

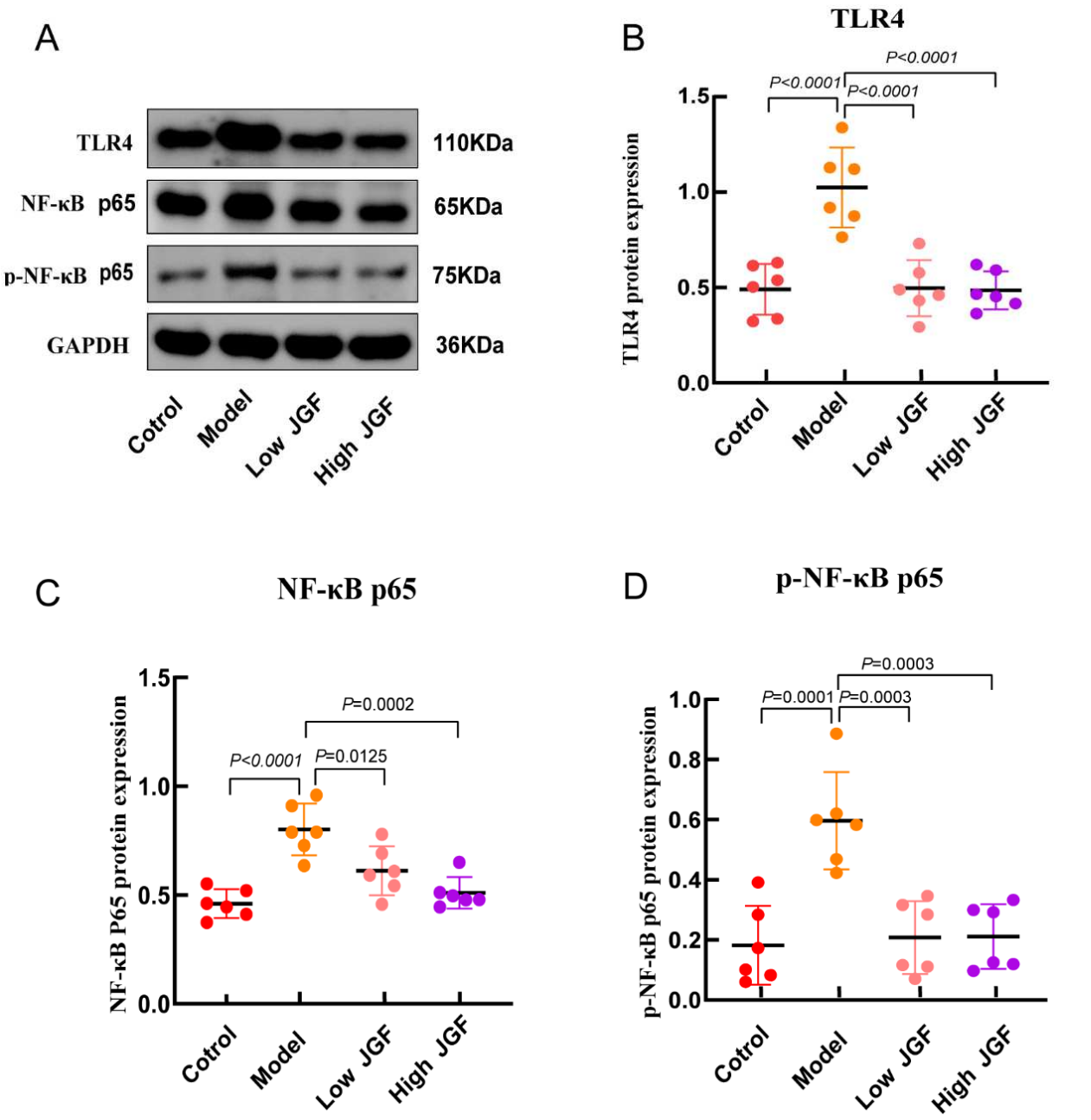

Fig. 4: Effect of JGF on the expression of TLR4, NF-κB p65, p-NF-κB p65 proteins in the liver of ALD rats. (A) The expression level of TLR4, NF-κB p65, p-NF-κB p65. (B) The relative expression of TLR4. (C) The relative expression of NF-κB p65. (D) The relative expression of p-NF-κB p65. All data are presented as mean ± SD (n=6) and analyzed via the ordinary one-way ANOVA combined with Tukey's multiple comparisons test. A value of $P < 0.05$ indicates the presence of significant difference.

Notably, JGF intervention effectively normalized the plasma and hepatic concentrations of these biomarkers. Therefore, JGF may exert hepatoprotective effects by reinforcing the stability of mitochondrial membranes and preserving cellular homeostasis, thereby mitigating alcohol-induced oxidative injury to hepatocytes.

TNF-α, IL-1β and IL-6 are principal mediators orchestrating systemic inflammatory responses. TNF-α emerges as the primary inflammatory initiator that can activate neutrophil and lymphocyte, modulating vascular endothelial permeability, regulating metabolism in peripheral tissues, stimulating secondary cytokine production, etc. Concurrently, IL-1β and IL-6 can facilitate lymphocyte proliferation and differentiation and upregulate endothelial adhesion molecules to amplify the inflammatory signaling (Mustafa *et al.*, 2021).

In our experiments, the observed significantly elevated circulating TNF-α, IL-1β and IL-6 concentrations after modeling corroborated previous findings that ethanol-induced hepatic damage would trigger systemic inflammatory responses (Zhao *et al.*, 2021). Notably, JGF administration effectively attenuated pro-inflammatory cytokine levels in both plasma and hepatic tissues of ALD models, indicating its potent anti-inflammatory properties. Thus, JGF may exert hepatoprotective function through modulating inflammatory pathways. Based on its cytokine-regulating capacity, JGF can potentially benefit hepatic parenchymal regeneration, beyond its role of mitigating inflammation, indicating its dual therapeutic potential for liver pathologies. These findings warrant further mechanistic investigations to uncover the immunomodulatory properties of traditional botanical preparations in hepatic disorders.

As a key receptor for lipopolysaccharide (LPS) recognition, conventionally, TLR4 has been recognized to be a critical pattern recognition receptor predominantly expressed on macrophage membranes. It serves as a crucial mediator in innate immunity by recognizing pathogen-derived molecular motifs, particularly functioning as the principal receptor for bacterial LPS (Androutsakos *et al.*, 2022). LPS-mediated TLR4 triggering may activate signaling cascades that converge on NF-κB and interferon regulatory factor mobilization (Liu *et al.*, 2022). Furthermore, as a pivotal nuclear transcription factor, NF-κB governs the expression of numerous genes implicated in critical cellular processes such as programmed cell death, cellular growth, inflammatory responses and autoimmune pathogenesis (Song *et al.*, 2021). NF-κB has been confirmed to be significantly involved in hepatic pathologies, particularly in mediating inflammatory liver damage (Song *et al.*, 2022). Emerging evidence strongly supports the central involvement of TLR4/NF-κB signaling axis in the pathogenesis of ALD (Mai *et al.*, 2022; Hu *et al.*, 2025). In our study, bioactive constituents contained in JGF might effectively inactivate the TLR4/NF-κB pathway, potentially offering a novel pharmacological approach for ALD intervention via modulating the proposed signaling network.

In this study, the hepatoprotective effect of JGF against ethanol-induced chronic hepatic damage was discovered to be related to the regulation of the TLR4/NF-κB signaling cascade. JGF administration could potentiate endogenous antioxidant systems while optimizing the hepatic cellular microenvironment. More importantly, it effectively interrupts the pathogenic cascade of ALD at its origin. Mechanistically, JGF could suppress alcohol-triggered inflammatory responses via modulating the TLR4/NF-κB signaling pathway to attenuate ALD progression eventually. These integrated findings position JGF as a viable therapeutic option for ALD, supporting it as an innovative liver-protective compound on the basis of the yielded mechanistic and pharmacological evidence.

However, this study has several inherent limitations that should be considered with caution. Many traditional Chinese medicines, especially compound formulas, consist of various Chinese herbs, most of which originate from natural sources and possess complex chemical compositions. There was a lack of comprehensive chemical profiling to define the active constituents in this study, necessitating future work to establish a fingerprint for quality control and reproducibility by incorporating UPLC-MS analysis. At present, investigations within this field remain confined to initial rodent assessments, with further exploration required to validate the TLR4/NF-κB pathway in clinical contexts and to investigate the precise molecular mechanisms involved. Additionally, clinical trials are needed to provide clearer evidence of the efficacy and safety of this herbal formulation for managing ALD.

CONCLUSION

In conclusion, JGF exhibits therapeutic promise in ALD management. It can attenuate hepatic pathological alterations, enhance biochemical markers of liver function, mitigate oxidative damage and regulate inflammatory responses through modulation of the TLR4/NF-κB cascade. These compelling outcomes support its advancement as a novel botanical-based treatment strategy for hepatic disorders. However, these findings warrant additional mechanistic studies and clinical evaluation to fully elucidate the pharmacological actions and therapeutic potential of JGF.

Acknowledgment
This research was supported by Xiamen Natural Science Foundation Joint Project (No.3502Z202374109).

Author's contributions
Shuifang Chen drafted the manuscript and revised the final version. Xuemei Chen performed data curation and formal analysis. Liangong Peng conducted the investigation and animal experiments. Yihui Huang provided study resources and prepared the herbal decoction. Yiqing Lin and Yinglian Cai participated in the investigation and were responsible for data collection and detection. Qianwen Zheng conceptualized the study, acquired funding, provided supervision, and administered the project. All authors have reviewed and approved the final manuscript.

Funding
This work was supported by Xiamen Natural Science Foundation Joint Project（No.3502Z202374109).

Data availability statement
The authors declare that the data underlying the findings of this study are available from the corresponding author upon reasonable request.

Ethical approval
All procedures related to animal experiments were rigorously reviewed and approved by the Institutional

Animal Care and Use Committee (IACUC) of Fuzhou Cold-Spring Biology Co., LTD. (IACUC-BWS-P22024002).

Conflict of interest

The authors declare no competing interests.

REFERENCES

Androutsakos T, Bakasis AD, Pouliakis A, Gazouli M, Vallilas C and Hatzis G (2022). Single nucleotide polymorphisms of toll-like receptor 4 in hepatocellular carcinoma-A single-center study. *Int J Mol Sci.*, **23**(16): 9430.

Asrani SK, Mellinger J, Arab JP and Shah VH (2021). Reducing the global burden of alcohol-associated liver disease: A blueprint for action. *Hepatology*, **73**(5): 2039-2050.

Cao H, Xi S, He W, Ma X, Liu L, Xu J, Zhang K, Li Y and Jin L (2021). The effects of Gentiana dahurica Fisch on alcoholic liver disease revealed by RNA sequencing. *J Ethnopharmacol*, **279**: 113422.

Cao P, Chao X, Ni HM and Ding WX (2026). An update on animal models of alcohol-associated liver disease. *Am J Pathol,* **196**(1): 4-19.

Chen XF, Zhang JH, Li R, Zhang H, Sun Y, Jiang L, Wang XY and Xiong YK (2022). Flos Puerariae-Semen Hoveniae medicinal pair extract ameliorates DSS-induced inflammatory bowel disease through regulating MAPK signaling and modulating gut microbiota composition. *Front Pharmacol*, **13**: 1034031.

Chen Y, Gao T, Bai J, Yu L, Liu Y, Li Y, Zhang W, Niu S, Liu S and Guo J (2025a). Ge-Zhi-Jie-Jiu decoction alleviates alcoholic liver disease through multiple signaling pathways. *J Ethnopharmacol*, **337**(Pt 1): 118840.

Chen Y, Zhang D, Wu Y, Jiang W, Guo L, Pan D, He Q, Yin Z, Sun L and Wang S (2025b). Chronic intermittent hypoxia alleviates alcohol-related liver injury via downregulation of hepatic hypoxia-inducible factor-2α. *Am J Physiol Gastrointest Liver Physiol*, **328**(5): G610-g623.

Cho Y, Choi YI, Oh S, Han J, Joo SK, Lee DH, Jung YJ, Kim BG, Lee KL and Kim W (2020). Point shear wave elastography predicts fibrosis severity and steatohepatitis in alcohol-related liver disease. *Hepatol Int*, **14**(2): 270-280.

Farhadi S, Mohammadi S, Alkindi AY and Al-Amri IS (2025). Therapeutic potential of elafibranor in alcohol-associated liver disease: Insights into macrophage modulation and fibrosis reduction. *World J Biol Chem*, **16**(1): 104535.

Han W, Li H, Jiang H, Xu H, Lin Y, Chen J, Bi C and Liu Z (2023). Progress in the mechanism of autophagy and traditional Chinese medicine herb involved in alcohol-related liver disease. *PeerJ*, **11**: e15977.

Hu Y, Wang Y, Li X, Xie Q and Lyu Z (2025). Clostridium butyricum JJ100 and Lacticaseibacillus rhamnosus LR alleviate liver injury in mice caused by continuous high-dose-alcohol exposure by protecting the intestinal barrier, rebuilding the gut microbiota and regulating AMPK and TLR4/NF-κB signaling pathways. *Food Funct*, **16**(16): 6687-6702.

Huang DQ, Mathurin P, Cortez-Pinto H and Loomba R (2023). Global epidemiology of alcohol-associated cirrhosis and HCC: Trends, projections and risk factors. *Nat Rev Gastroenterol Hepatol*, **20**(1): 37-49.

Jiang YH, Wang L, Chen WD, Duan YT, Sun MJ, Huang JJ, Peng DY, Yu NJ, Wang YY and Zhang Y (2022). *Poria cocos* polysaccharide prevents alcohol-induced hepatic injury and inflammation by repressing oxidative stress and gut leakiness. *Front Nutr*, **9**: 963598.

Jin YL, Wang CY, Meng ZQ, Zhang YX, Meng DS, Liu JQ, Yuan M and Guan S (2025). Proanthocyanidins alleviate acute alcohol liver injury by inhibiting pyroptosis via inhibiting the ROS-MLKL-CTSB-NLRP3 pathway. *Phytomedicine,* **136**: 156268.

Kong EQZ, Subramaniyan V and Lubau NSA (2024). Uncovering the impact of alcohol on internal organs and reproductive health: Exploring TLR4/NF-kB and CYP2E1/ROS/Nrf2 pathways. *Animal Model Exp Med*, **7**(4): 444-459.

Laschtowitz A, Zachou K, Lygoura V, Pape S, Derben F, Jaeckel E, Oller-Moreno S, Weidemann S, Krech T, Piecha F, Schön G, Liebhoff AM, Al Tarrah M, Heneghan M, Drenth JPH, Dalekos G, Taubert R, Lohse AW and Schramm C (2021). Histological activity despite normal ALT and IgG serum levels in patients with autoimmune hepatitis and cirrhosis. *JHEP Rep*, **3**(4): 100321.

Lee JA, Shin MR, Park HJ and Roh SS (2022). Scutellariae radix and citri reticulatae pericarpium mixture regulate PPARγ/RXR signaling in reflux esophagitis. *Evid Based Complement Alternat Med*, **2022**: 6969241.

Li M, Wei ZC, Zhang FX and Li HJ (2025). Phytochemical analysis of semen hoveniae and its potential mechanism against alcoholic liver disease via an integrated approach combining UHPLC-Q-TOF MS, network pharmacology and molecular docking. *Rapid Commun Mass Spectrom*, **39**(20): e10097.

Liu ZN, Wu X, Fang Q, Li ZX, Xia GQ, Cai JN and Lv XW (2022). CD73 attenuates alcohol-induced liver injury and inflammation via blocking TLR4/MyD88/NF-κB signaling pathway. *J Inflamm Res*, **15**: 53-70.

Mai B, Han L, Zhong J, Shu J, Cao Z, Fang J, Zhang X, Gao Z and Xiao F (2022). Rhoifolin alleviates alcoholic liver disease *in-vivo* and *in-vitro* via inhibition of the TLR4/NF-κB signaling pathway. *Front Pharmaco*l, **13**: 878898.

Moustafa PE, Farouk H, Khattab MS and El-Marasy SA (2025). Diacerein counteracts amiodarone-induced hepatotoxicity in rats via targeting TLR4/NF-kB/NLRP3 pathways. *Toxicol Mech Methods*, **35**(7):

787-799.

Mustafa G, Mahrosh HS and Arif R (2021). *In silico* characterization of growth differentiation factors as inhibitors of TNF-Alpha and IL-6 in immune-mediated inflammatory disease rheumatoid arthritis. *Biomed Res Int*, **2021**: 5538535.

Song X, Cui W, Meng F, Xia Q, Li X, Hou M, Jia L and Zhang J (2022). Glucopyranose from Pleurotus geesteranus prevent alcoholic liver diseases by regulating Nrf2/HO-1-TLR4/NF-κB signalling pathways and gut microbiota. *Food Funct*, **13**(5): 2441-2455.

Song X, Sun W, Cui W, Jia L and Zhang J (2021). A polysaccharide of PFP-1 from Pleurotus geesteranus attenuates alcoholic liver diseases via Nrf2 and NF-κB signaling pathways. *Food Funct*, **12**(10): 4591-4605.

Su P, Qiu H, Liang L, Weng L, Liu Y, Liu J, Wu L and Meng F (2024). The antioxidant activity of polysaccharides from Armillaria gallica. *Front Nutr*, **11**: 1277877.

Toto A, Wild P, Graille M, Turcu V, Crézé C, Hemmendinger M, Sauvain JJ, Bergamaschi E, Guseva Canu I and Hopf NB (2022). Urinary malondialdehyde (MDA) concentrations in the general population-A systematic literature review and meta-analysis. *Toxics*, **10**(4): 160.

Wang H, Bian Y, Li Y, Yuan Y, Li X, Liu Y and Wang X (2025). Echinacoside: A potential therapeutic approach for alcohol-related liver disease by alleviating intestinal microbial dysbiosis, intestinal barrier dysfunction and liver inflammation mediated by the endotoxin-TLR4/NF-κB pathway. *Eur J Pharmacol*, **1005**: 178027.

Yang YM, Cho YE and Hwang S (2022). Crosstalk between oxidative stress and inflammatory liver injury in the pathogenesis of alcoholic liver disease. *Int J Mol Sci*, **23**(2): 774.

Yeh YT, Wu X, Ma Y, Ying Z, He L, Xue B, Shi H, Choi Y and Yu L (2023). Single ethanol binge causes severe liver injury in mice fed Western diet. *Hepatol Commun*, **7**(7): e00174.

Yoo JJ, Lee DH, Chang Y, Jo H, Cho YY, Lee S, Kim LY and Jang JY (2024). Trends in alcohol use and alcoholic liver disease in South Korea: A nationwide cohort study. *BMC Public Health*, **24**(1): 1841.

Zhang H, Wei Z, Tong Y, Song X, Li S, Sun Y, Liu C, Han F and Yu J (2023). Spectrum-effect relationship study to reveal the pharmacodynamic substances in Flos Puerariae-Semen Hoveniae medicine pair for the treatment of alcohol-induced liver damage. *J Ethnopharmacol*, **314**: 116628.

Zhang XM, Huang YC, Chen BZ, Li Q, Wu PP, Chen WH, Wu RH and Li C (2024). Water decoction of Pericarpium citri reticulatae and Amomi fructus ameliorates alcohol-induced liver disease involved in the modulation of gut microbiota and TLR4/NF-κB pathway. *Front Pharmaco*l, **15**: 1392338.

Zhao L, Mehmood A, Soliman MM, Iftikhar A, Iftikhar M, Aboelenin SM and Wang C (2021). Protective effects of ellagic acid against alcoholic liver disease in mice. *Front Nutr*, **8**: 744520.

Zhou X, Wang J and Zhou S (2024). Poria cocos polysaccharides improve alcoholic liver disease by interfering with ferroptosis through NRF2 regulation. *Aging (Albany NY)*, **16**(7): 6147-6162.